

Figure 1. Design and readout of Polycomb *in-vivo* Assay. Related to Figure 1. **A.** An array of DNA binding sites including 12 x ZFHD1 and 4 x Gal4 UAS are located upstream of an EF1alpha promoter controlling constitutive expression of a GFP reporter gene. 12 x ZFHD1 DNA binding sites facilitate recruitment of ZFHD1 alone or as a chimeric fusion with human CBX7. **B.** Flow cytometry histogram shows GFP expression in response to expression of ZFHD1 alone (top) or ZFHD1-CBX7 fusion (bottom). Percentage indicates fraction of GFP-positive reporter mESCs. **C.** ChIP-qPCR analysis shows relative enrichment (Bound/Input) of CBX7, RING1B and H2AK119ub1 in response to ZFHD1 alone or ZFHD1-CBX7 tethering. ChIP-qPCR for H2AK119ub1 is normalized to IAP. IAP serves as negative control and Evx2 as positive control. **D.** Small molecule antagonism of propagation of Polycomb-mediated silencing in a separate TetOFF reporter cell line (Moussa et al., 2019). Treatment with control compound (UNC4219) does not impair maintenance of CBX7-induced GFP reporter gene silencing. In contrast, heritable silencing after Dox-induced TetR-CBX7 release is decreased in response to UNC3866 or UNC4976. Percentage of cells maintaining GFP silencing after six days of Dox treatment in response to increasing concentrations of CBX7 antagonists (UNC3866, UNC4976) or control compound (UNC4219). Data in **C** and **D** are presented as mean \pm SD from two replicate experiments.

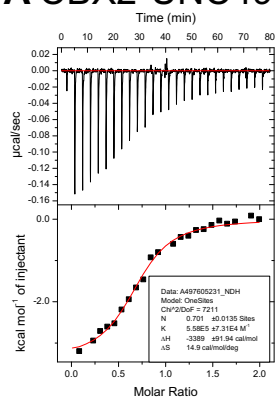
Isothermal Titration Calorimetry (ITC) Affinity Data		
Protein	UNC3866 ITC K _d (μM)	UNC4976 ITC K _d (μM)
CBX2	1.800 ± 0.210 (n=2)	1.665 ± 0.177 (n=2)
CBX4	0.094 ± 0.017 (n=2)	0.062 ± 0.004 (n=2)
CBX6	0.610 ± 0.008 (n=2)	0.561 ± 0.175 (n=2)
CBX7	0.097 ± 0.003 (n=2)	0.059 ± 0.018 (n=4)
CBX8	1.200 ± 0.021 (n=2)	n.d.*
CDYL2	0.850 ± 0.076 (n=2)	0.459 ± 0.123 (n=2)

Table 1. ITC Data Comparison for UNC3866 and UNC4976. Related to Figure 1. Data are presented as mean ± SD from at least two replicate experiments (n), *not stable in presence of DMSO required for UNC4976 solubilization.

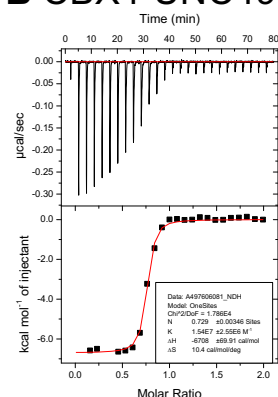
Surface Plasmon Resonance (SPR) Kinetic Data		
CBX2		
	Residence Time (1/k _d) (s)	K _d (nM)
UNC4195	53.2	1020.0
UNC5355	34.4	1750.0
CBX4		
	Residence Time (1/k _d) (s)	K _d (nM)
UNC4195	46.7	28.3
UNC5355	50.3	26.7
CBX6		
	Residence Time (1/k _d) (s)	K _d (nM)
UNC4195	14.5	642.0
UNC5355	15.5	543.0
CBX7		
	Residence Time (1/k _d) (s)	K _d (nM)
UNC4195	56.2	42.0
UNC5355	46.1	53.8
CBX8		
	Residence Time (1/k _d) (s)	K _d (nM)
UNC4195	28.0	415.0
UNC5355	27.4	458.0
CDYL2		
	Residence Time (1/k _d) (s)	K _d (nM)
UNC4195	8.3	698.0
UNC5355	14.2	415.0

Table 2. SPR Data Comparison for biotinylated UNC3866 (UNC4195) and UNC4976 (UNC5355). Related to Figure 1. For each of the six chromodomains tested, residence time is reported as the inverse of the off-rate (k_d) and kinetic dissociation constants (K_d's) are reported and calculated from both kinetic on-rates (k_a) and off-rates (k_d) (K_d = k_d/k_a).

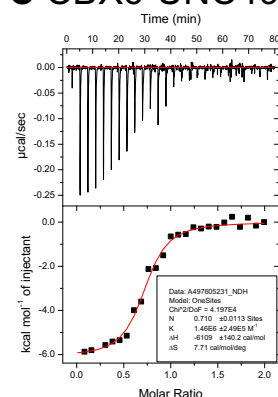
A CBX2-UNC4976



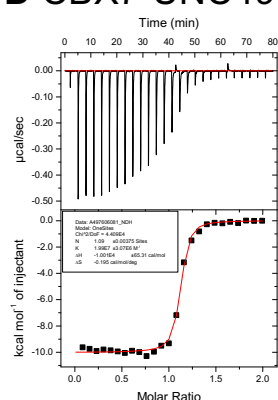
B CBX4-UNC4976



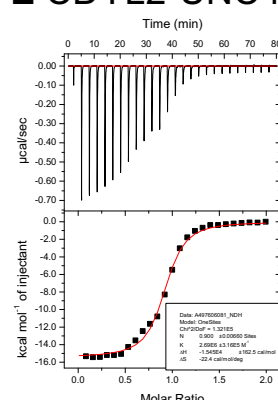
C CBX6-UNC4976



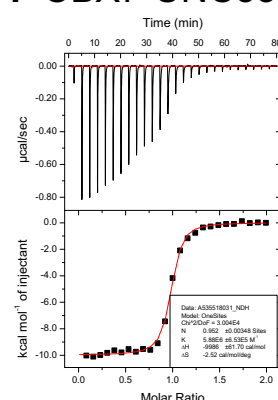
D CBX7-UNC4976



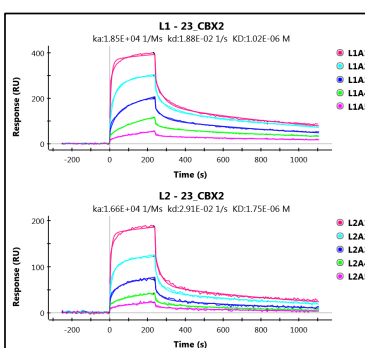
E CDYL2-UNC4976



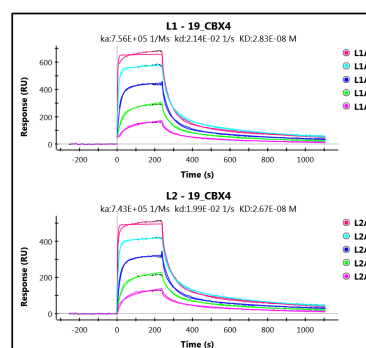
F CBX7-UNC5355



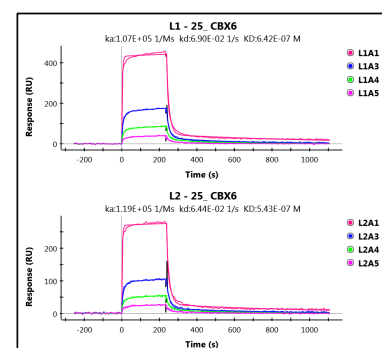
G



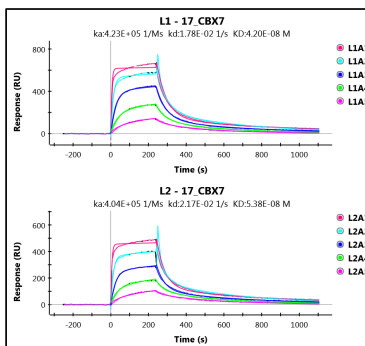
H



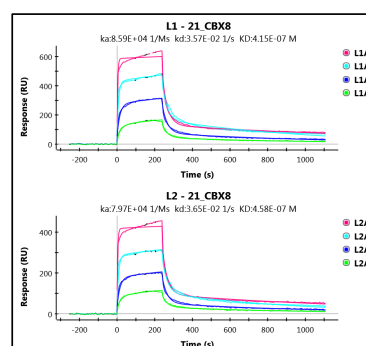
I



J



K



L

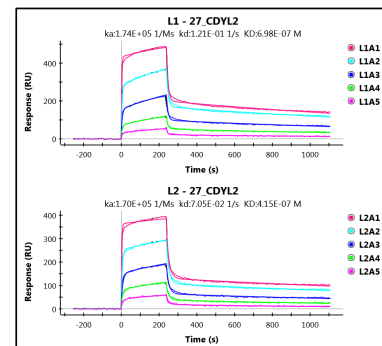
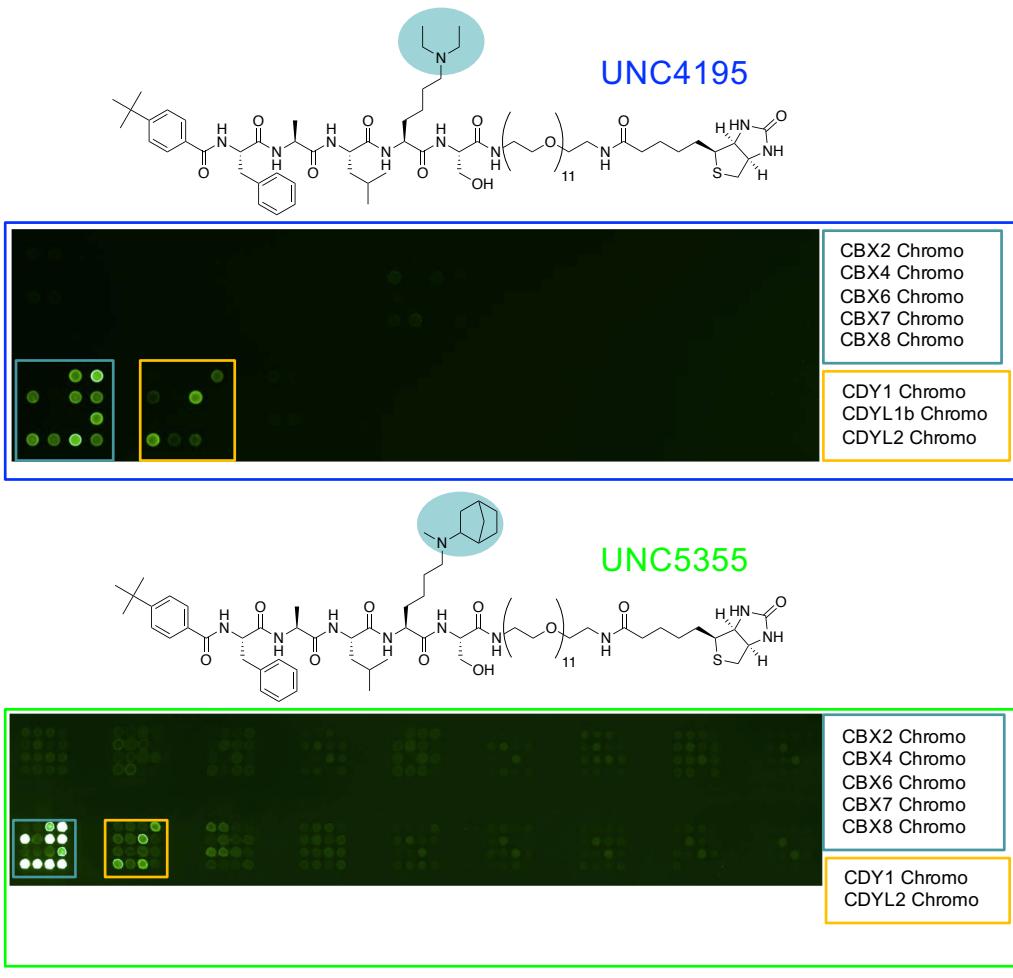


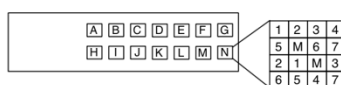
Figure 2. Representative Data from Biophysical Experiments. Related to Figure 1. A-F. Representative Isothermal Titration Calorimetry (ITC) curves for all chromodomains tested with UNC4976 (**A-E**), and CBX7 tested with UNC5355 (**F**). **G-L.** Surface Plasmon Resonance (SPR) Sensorgrams from Kinetic Experiments. Sensorgrams for CBX2 (**G**), CBX4 (**H**), CBX6 (**I**), CBX7 (**J**), CBX8 (**K**), and CDYL2 (**L**) are shown. For each protein, UNC4195 data is shown on the top sensorgram and UNC5355 data is shown on the bottom sensorgram.

A



B

Biomatik Full Array 3



TUDOR	TUDOR	TUDOR	TUDOR	TUDOR	TUDOR-PHD	PHD
A1) S3BP1(-1)	B1) TDRD8	C1) TDPS6	D1) SETDB1	F1) JMD2/B	G1) KNG2	
A2) S3BP1(-1)*	B2) TDRD4-3	C2) TDPS9	D2) SMN1	F2) SETDB2/C	G2) TAF9	
A3) TDRD1-2	B3) TDRD4	C3) TDPS10	D3) PHF1	F3) MTIF2	G3) TRIM24 ^a	
A4) TDRD1-3	B4) TDRD5	C4) TDPS11	D4) PHF19	E4) SPF30	F4) CHD5(1'-2)*	
A5) TDRD1-4	B5) TDRD6-5	C5) TDPS12-1	D5) PHF20	E5) UHFR1	F5) CHD6	CHROMOPHOBIN
A6) TDRD2	B6) TDRD6-6	C6) ARID4A	D6) PHF20-2	E6) ZPAT8	F6) PomBa1*	G6) CHD3
A7) TDRD3	B7) TDRD6-7	C7) ARID4B	D7) PHF20L1	E7) JMJD2A(1-2)	F7) Spindlin1*	G7) CHD4
<hr/>						
CHROMO	CHROMO	CHROMO	CHROMO	AGENET	IDCL	BBMO
A1) ARID4A	B1) ARID4B	C1) CHD1	D1) FMR1	E1) PCNA	F1) SP140*	G1) BBMO
A2) ARID4B	B2) CHD1	C2) CHD2	D2) FXR1	E2) PCNA	F2) SP140(1')	G2) BBMO
A3) CBX2	B3) CBX3	C3) CBX3	D3) MYST1/MOF	M1) LMBTL1(1-3)	M2) LMBTL1(1-3)*	N1) WDRN(1-2)*
A4) CBX4	B4) CDY1	C4) CHD7	D4) SMARCC1	M3) LMBTL1(1-3)*	M4) SMAP2	N2) WDRN(1-3)
A5) CBX6	B5) CDYL1b	C5) CHD8	D5) SMARCC2	L4) GLP	P1) WDRN2	HEAT
A6) CBX7	B6) CDYL2	C6) CHD9	D6) SUV39H1	L5) IKB FL2	M6) DNMT3A	N3) NAP-303(1-4)
A7) CBX8	B7) MSL3	C7) TIPE6	D7) SUV39H2	B1) NS1	M7) NS1	N4) NAP-305(1-4)
<hr/>						
CHROMO	CHROMO	CHROMO	CHROMO	AGENET	IDCL	BBMO
A1) CHD1	B1) CHD1	C1) CHD1	D1) FMR1	E1) PCNA	F1) SP140*	G1) BBMO
A2) CHD2	B2) CHD1	C2) CHD2	D2) FXR1	E2) PCNA	F2) SP140(1')	G2) BBMO
A3) CHD3	B3) CHD2	C3) CHD3	D3) MYST1/MOF	M1) LMBTL1(1-3)	M2) LMBTL1(1-3)*	N1) WDRN(1-2)*
A4) CHD7	B4) CHD7	C4) CHD7	D4) SMARCC1	M3) LMBTL1(1-3)*	M4) SMAP2	N2) WDRN(1-3)
A5) CHD8	B5) CHD8	C5) CHD8	D5) SMARCC2	L4) GLP	P1) WDRN2	HEAT
A6) CHD9	B6) CHD9	C6) CHD9	D6) SUV39H1	L5) IKB FL2	M6) DNMT3A	N3) NAP-303(1-4)
A7) TIPE6	B7) MSL3	C7) TIPE6	D7) SUV39H2	B1) NS1	M7) NS1	N4) NAP-305(1-4)
<hr/>						
TUDOR	TUDOR	TUDOR	TUDOR	TUDOR	TUDOR-PHD	PHD
A1) S3BP1(-1)	B1) TDRD8	C1) TDPS6	D1) SETDB1	F1) JMD2/B	G1) KNG2	
A2) S3BP1(-1)*	B2) TDRD4-3	C2) TDPS9	D2) SMN1	F2) SETDB2/C	G2) TAF9	
A3) TDRD1-2	B3) TDRD4	C3) TDPS10	D3) PHF1	F3) MTIF2	G3) TRIM24 ^a	
A4) TDRD1-3	B4) TDRD5	C4) TDPS11	D4) PHF19	E4) SPF30	F4) CHD5(1'-2)*	
A5) TDRD1-4	B5) TDRD6-5	C5) TDPS12-1	D5) PHF20	E5) UHFR1	F5) CHD6	CHROMOPHOBIN
A6) TDRD2	B6) TDRD6-6	C6) ARID4A	D6) PHF20-2	E6) ZPAT8	F6) PomBa1*	G6) CHD3
A7) TDRD3	B7) TDRD6-7	C7) ARID4B	D7) PHF20L1	E7) JMJD2A(1-2)	F7) Spindlin1*	G7) CHD4

C

Methyl Domain Readers Array - BFA5

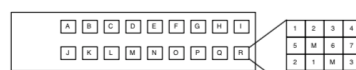


Figure 3. Reader Domain Protein Microarray Selectivity Data Comparison with Biotinylated Compounds.

Related to Figure 1. **A.** Protein microarray data for UNC4195 (top) and UNC5355 (bottom) with bound proteins highlighted in teal and yellow boxes. **B.** Complete list of histone reader domains evaluated on the protein microarray screened against UNC4195. Mapping of individual reader domains is described by the legend in the top right corner. **C.** Complete list of histone reader domains evaluated on the protein microarray screened against UNC5355. Mapping of individual reader domains is described by the legend in the top right corner. Boxes A-G and J-P are identical to the microarray described in (B), additional domains screened against UNC5355 but not UNC4195 are described in boxes H, I, Q and R.

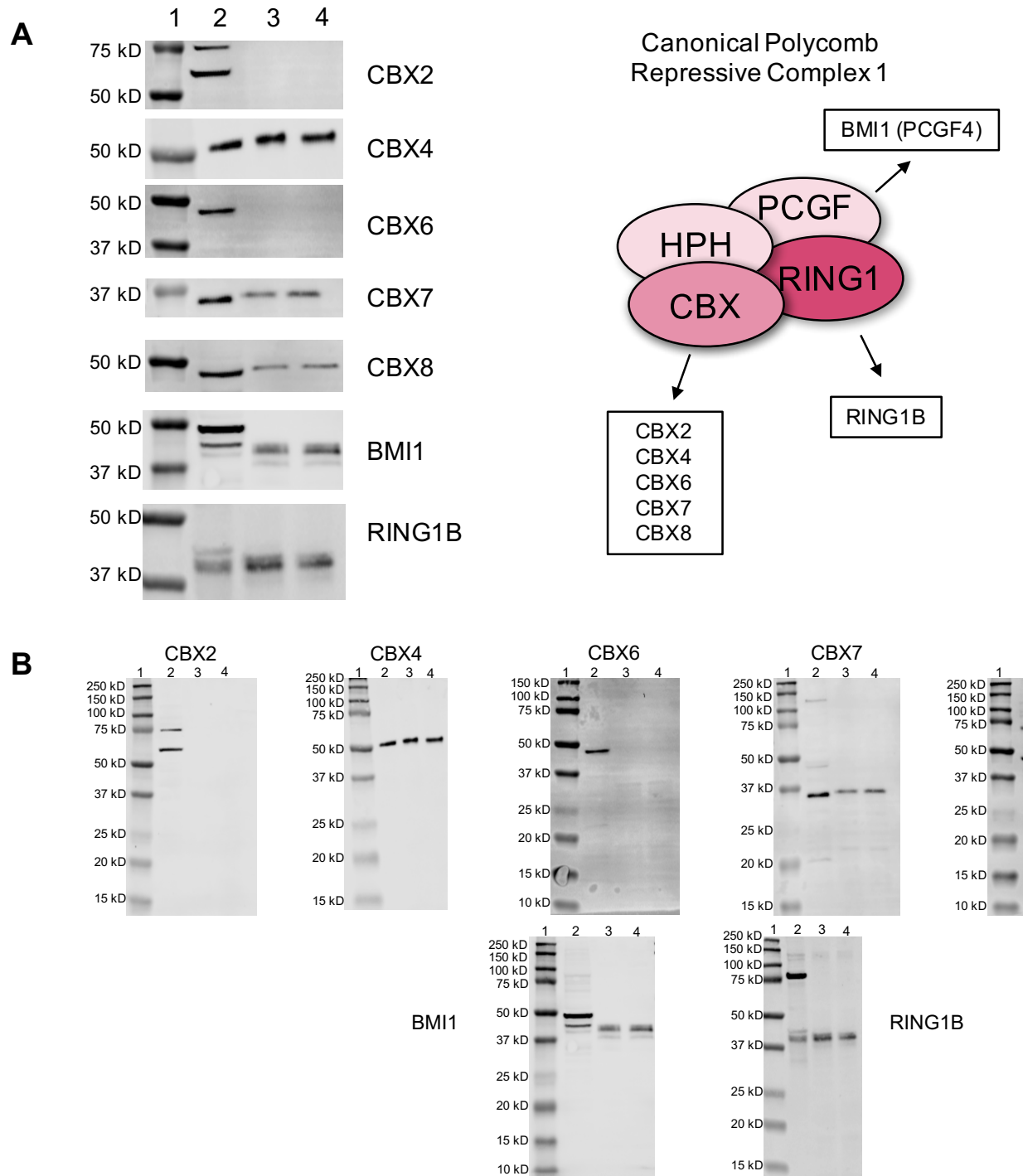


Figure 4. PC3 Lysate Pulldown Experiments with UNC4195 and UNC5355 Biotinylated Ligands. Related to Figure 1. A. (Left) Cropped blots highlighting bands of interest from PC3 lysate pulldowns with biotinylated ligands. (Right) Canonical PRC1 complex, with immunoblotted subunits listed. **B.** Uncropped western blots for individual proteins. For all blots in **A** and **B**, Lane 1= BioRad Precision Plus Protein Dual Color Standards (#1610374), Lane 2= PC3 Lysate Input, Lane 3= UNC4195 pulldown, and Lane 4= UNC5355 pulldown. Western blots shown are representative of three replicate experiments.

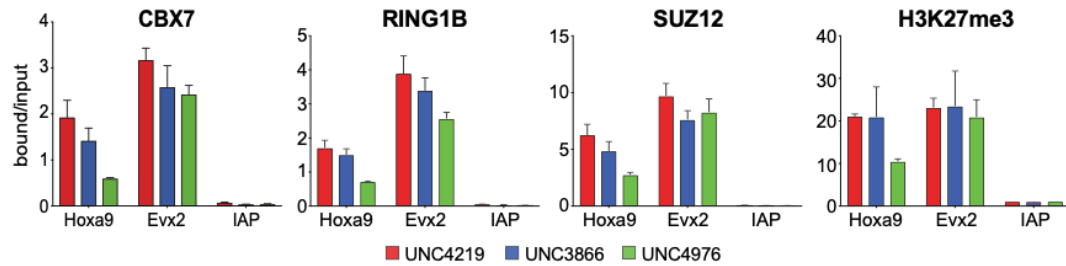
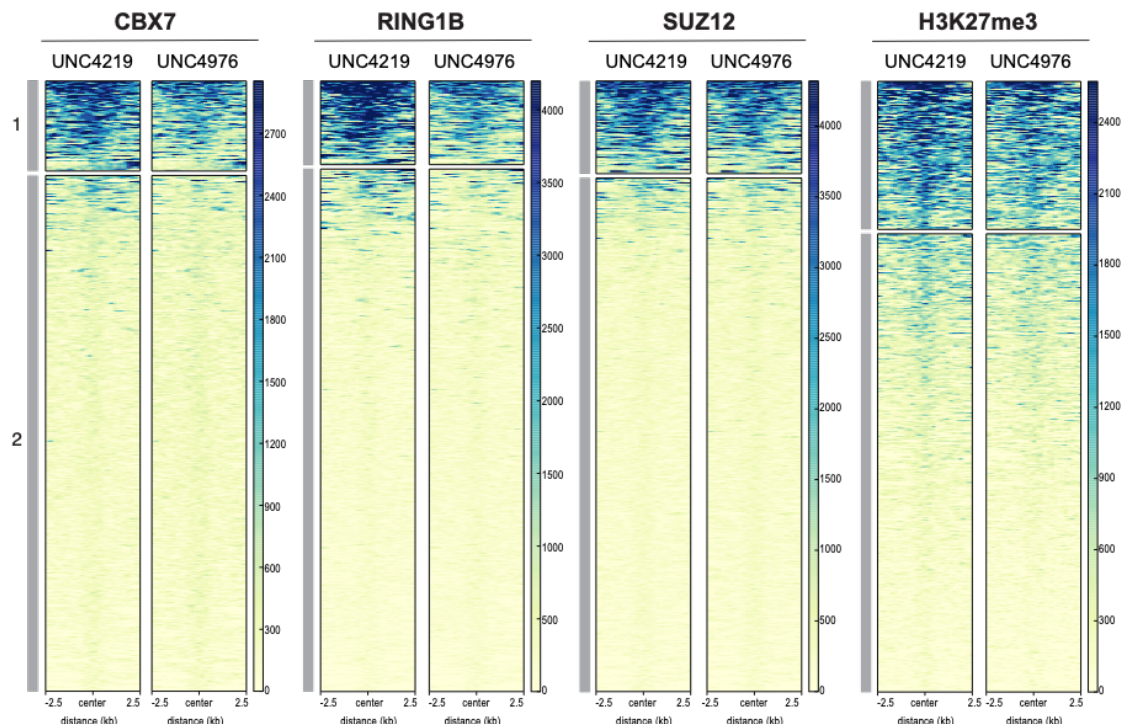
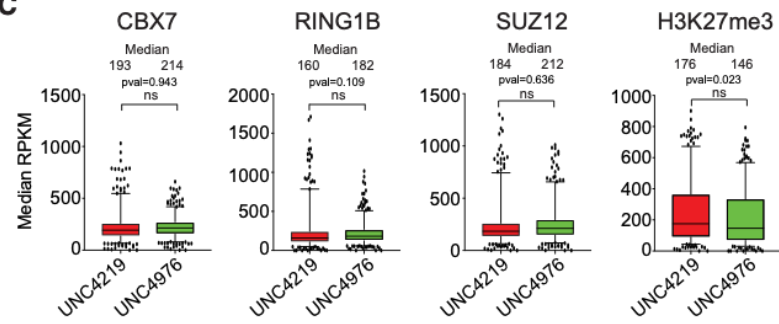
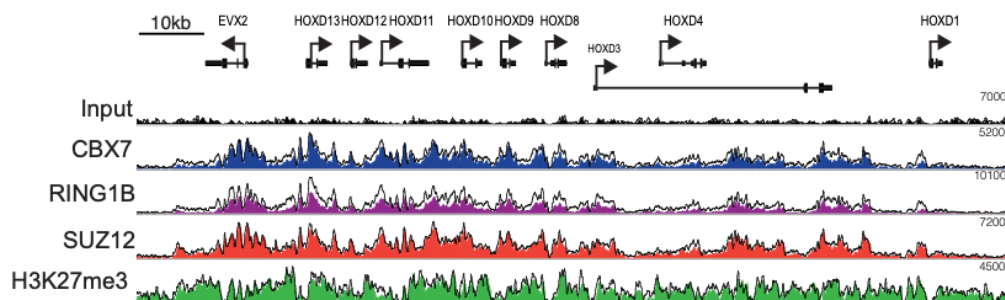
A**B****C****D**

Figure 5. UNC4976 efficiently displaces CBX-containing PRC1 from Polycomb target genes. Related to Figure 3. **A.** ChIP-qPCR analysis shows relative enrichment of CBX7, RING1B, SUZ12 and H3K27me3 at selected genes in mES cells treated for 4hrs with 20 μ M of control compound UNC4219 (red), UNC3866 (blue) or UNC4976 (green). IAP serves as negative control. Analysis of H3K27me3 is normalized to IAP. Data are presented as mean \pm SD from at least two replicate experiments. **B.** Heat maps showing enrichment of capture ChIP-seq for CBX7, RING1B, SUZ12 and H3K27me3 in mES cells treated for 4hrs with 20 μ M of control compound UNC4219 or UNC4976. Signal is centered around peaks +/- 2.5 kb and plotted as FPKM normalized mapped reads and separated into “high” (1) and “low” (2) clusters. **C.** Boxplots of heat maps from capture ChIP-seq (**B**) show median RPKM normalized mapped reads of CBX7, RING1B, SUZ12 and H3K27me3 in “low” cluster (2). Statistical significance was calculated using unpaired t-test ($pval < 0.01$). **D.** Screenshots of capture ChIP-seq enrichment at HoxD cluster for RING1B, CBX7, SUZ12 and H3K27me3. Capture ChIP-seq signal of control UNC4219 treatment is shown as an outlined line and UNC4976-treated capture ChIP-seq samples are shown in filled color tracks. All data in A-D are representative of at least two independent biological replicates.

ChIP-qPCR Primer Sequences		
Gene	Forward Sequence	Reverse Sequence
HoxA9	GGATAATCGCCTAGGTGTGACTTAG	CATCTCTTGCCTCTCTGGG
Evx2	CGCAGCCCATCATTAAGAC	CGGACAAACTGGAGAACCTC
IAP	CTCCATGTGCTCTGCCTTCC	CCCCGTCCCTTTTAGGAGA

Table 3. ChIP-qPCR Primer Sequences. Related to Figure 3. Primer sequences for select Polycomb target genes used for ChIP-qPCR.

Capture-ChIP-seq Capture Probe Sequences						
Baits mm9 G11D genome			25 regions	genomic size		Polycomb target genes
chr1	4460681	4511256	Sox17	51	kb	y
chr1	17995977	18046157	Intergenic Crisp4	50	kb	m
chr2	74450084	74651064	Hoxd cluster	201	kb	y
chr2	105488775	105539252	Pax6	50	kb	y
chr2	153432137	153522909	Commd7&Dnmt3b	91	kb	n
chr3	34537459	34568988	Sox2	32	kb	n
chr3	87931198	88031358	Mef2d	100	kb	y
chr3	127332802	127342995	Neurog2	10	kb	y
chr4	88905858	88962573	Cdkn2a&b&Gm12610	57	kb	y
chr4	124294578	124395096	Pou3f1	101	kb	y
chr5	98563339	98814815	Prdm8&Fgf5&1700007G11Rik	251	kb	y
chr5	120094791	120194420	Tbx3	100	kb	n
chr6	122642090	122677539	Nanog	35	kb	n
chr7	110957144	111008233	Hbb locus	51	kb	n
chr7	137983359	138081333	Plekha1&Htra1	98	kb	n/m
chr7	149758083	149858985	Igf2&H19	101	kb	y
chr8	44361316	44426512	Zfp42	65	kb	n
chr9	89592758	89602918	Tmed3	10	kb	n
chr11	118870869	118961636	Cbx2/4/8	91	kb	y
chr12	87761185	87877500	Esrrb	116	kb	y
chr14	49256167	49306303	Otx2	50	kb	y
chr15	78819673	78905009	G11D locus	85	kb	n
chr16	91199329	91300463	Olig1&2	101	kb	y
chr17	35623948	35666758	Oct4/Pouf51 locus	43	kb	n
chr17	50414245	50444405	Dazl	30	kb	n

Table 4. Capture-ChIP-seq Probe Sequences. Related to Figure 3. Probe sequences for select Polycomb target genes used for Capture-ChIP-seq.

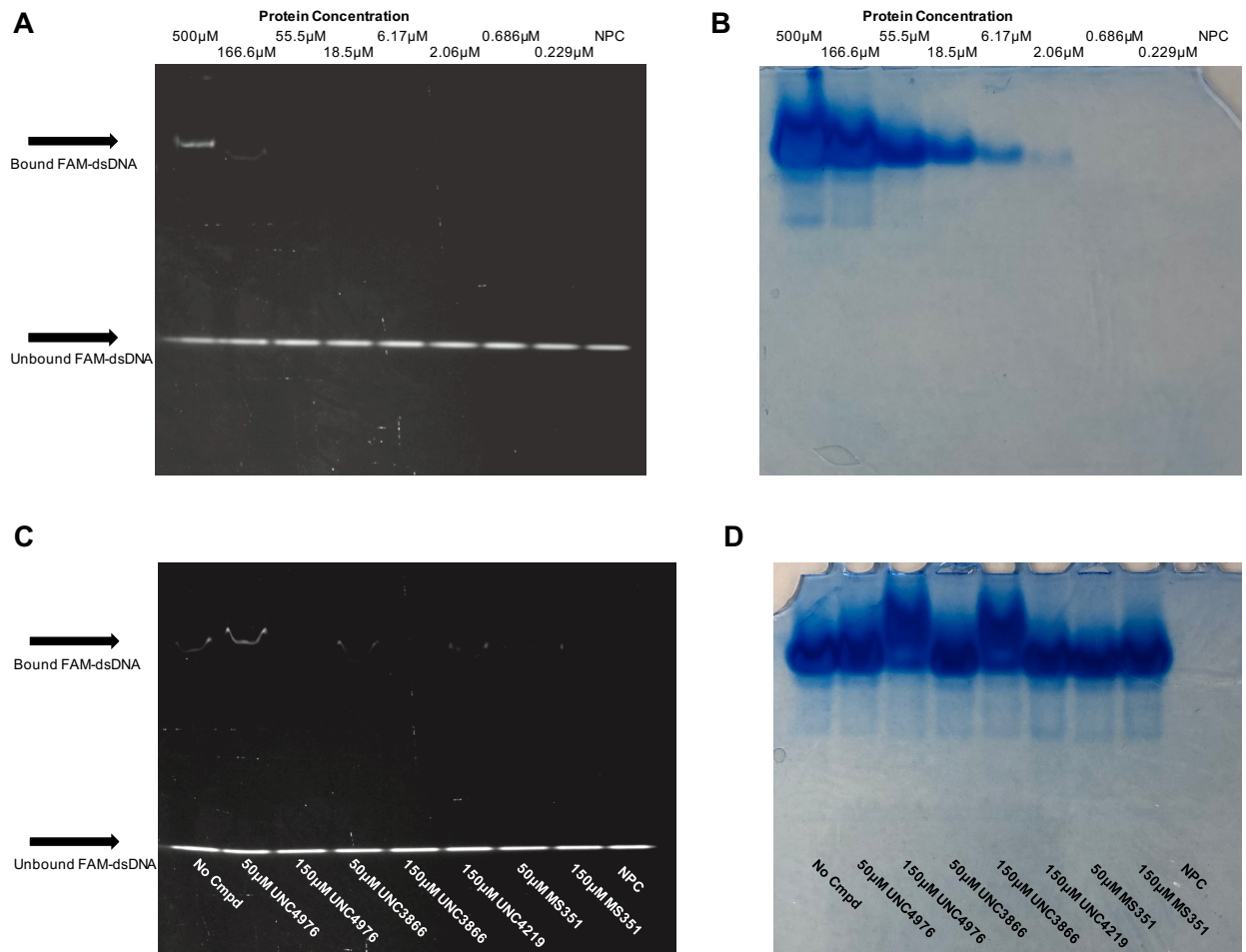


Figure 6. Electrophoretic Mobility Shift Assay (EMSA). Related to Figure 4. **A.** Fluorescent image of EMSA protein titration of CBX7 chromodomain with 100nM of FAM-dsDNA, demonstrating that CBX7 weakly binds FAM-dsDNA at 166 μ M. **B.** Follow up Coomassie staining of Tris-Glycine gel from **A**, demonstrating protein titration of CBX7 chromodomain. **C.** Fluorescent image of EMSA demonstrating that UNC4976 enhances the ability of CBX7 chromodomain to bind to FAM-dsDNA at a 1:3 ratio of compound to protein. All compounds were tested at either 1:3 or 1:1 ratios of compound to protein. **D.** Follow up Coomassie staining of Tris-Glycine gel from **C**, demonstrating that only UNC4976 and UNC3866 bind to CBX7 chromodomain as indicated by band shift. Images are representative of three replicate experiments.

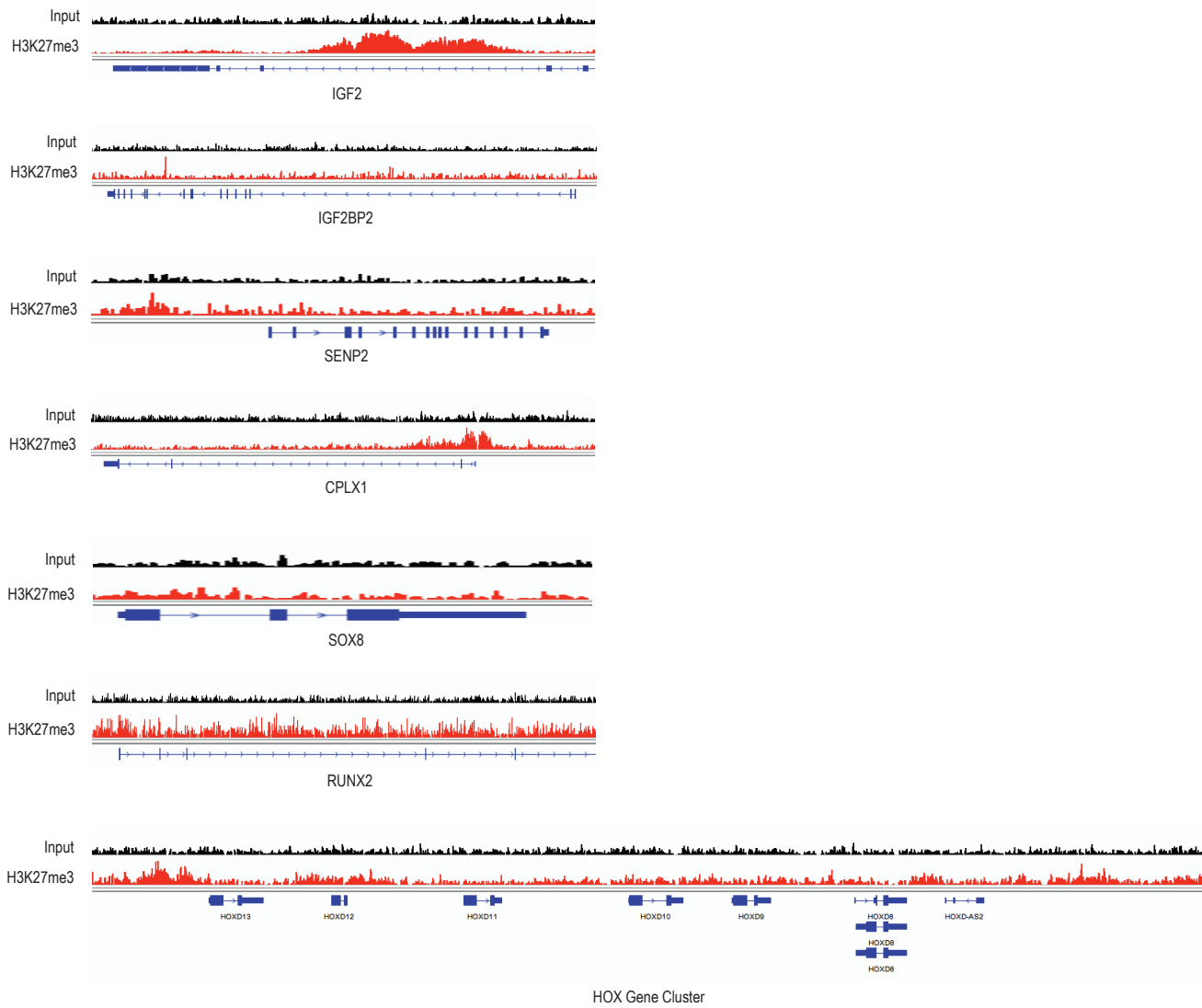


Figure 7. HEK293 Cells H3K27me3 ChIP-seq Data. Related to Figure 6. IGV Views showing H3K27me3 ChIP-seq signals from HEK293 cells (GEO: GSE133391) identifying PRC1 targets that were examined by RT-qPCR.

HEK293 RT-qPCR Primer Sequences		
Gene	Forward Sequence	Reverse Sequence
GAPDH	AACATCATCCCTGCCTCTACTGG	GTTTTCTAGACGGCAGGTCAAGG
HOXA1	CCAGGCCACCAAGAAGCCTGT	CCAGTTCCGTGAGCTGCTTG
HOXA4	CGTGGTGTACCCCTGGATGA	AAGACCTGCTGCCGGGTGTA
HOXC13	TCATCCCCGTCGAAGGCTAC	TGTAGGGCACCGCTTCTTG
HOXD9	GGCTGTTCGCTGAAGGAGGA	TCTCCAGCTCAAGCGTCTGGT
CPLX1	GTGTGAGTTCTGACCCCTGG	TCTGGTCCTTCTCCTCGTC
SOX8	GAGCTTGGCAACCGAAAACC	TGCTTCCAAACCCCAAACCT
RUNX2	CGCCTCACAAACAACCAACAG	GACTCTGTTGGTCTCGGTGG
CEBPD	CAACCAGGAGATGCAGCAGA	CAGCTGCTTGAAGAACTGCC
IGF2	AGTCGTGGCTCTCCATCTTG	CAGGCACAGGTGACATTGAG
IGFBP2	AAAACGGAGAGTGCTTGGGT	AGCAAGAAGGAGCAGGTGTG

Table 5. RT-qPCR Primer Sequences. Related to Figure 6. Primer sequences for select Polycomb target genes used for RT-qPCR in HEK293 cells.